15th Australasian Fluid Mechanics Conference
The University of Sydney, Sydney, Australia
13-17 December 2004

Small-Scale Turbulence: How Universal Is It?

R.A. Antonia and P. Burattini

Discipline of Mechanical Engineering
University of Newcastle, NSW, 2308 AUSTRALIA

Abstract

Kolmogorov's similarity hypotheses and his 4/5 law are valid at very large Reynolds numbers. For flows encountered in the laboratory, the effect of a finite Reynolds number and of the inhomogeneity associated with the large scales can affect the behaviour of inertial range scales significantly. This paper focuses on the source of inhomogeneity in two types of flows, those which are dominated mainly by a decay of energy in the streamwise direction and those which are forced, usually through a continuous injection of energy at large scales. Results based on a parameterization of the second-order velocity structure function indicate that the normalized third-order structure function approaches 4/5 more rapidly for forced than for decaying turbulence. These trends are supported by measurements and numerical data in these two flow types.

Introduction

There is little doubt that the similarity hypotheses proposed by Kolmogorov [36] (or K41) and their subsequent revision ([38] or K62) have had a major impact on turbulence research (e.g., [11,13,26,47,49,50,58,61]). A fundamental element of these hypotheses is the assumption that the small scale motion, which includes the dissipative and inertial ranges, is isotropic. Also, K41 and K62 require that the Reynolds number is very large so that the small scale motion is independent of the invariably anisotropic large scale motion. The major outcome of the first similarity hypothesis is the prediction

$$\langle(\delta u^*)^n\rangle = f_{un}(r^*), \tag{1}$$

where the increment $\delta u \equiv u(x+r)-u(x)$ (u is the velocity fluctuation along x; the separation r is aligned with x, and the angular brackets denote averaging). For each value of n, f_{un} is a universal function, in the sense that it is expected to depend only on $r^* \equiv r/\eta$ ($\eta \equiv \left(\nu^3/\langle\varepsilon\rangle\right)^{1/4}$ is the Kolmogorov length scale, ν is the kinematic viscosity and $\langle\varepsilon\rangle$ is the mean energy dissipation rate). The asterisk denotes normalization by the Kolmogorov velocity scale $u_K \equiv \left(\nu\langle\varepsilon\rangle\right)^{1/4}$ and/or η. The second similarity hypothesis yields the famous inertial range ($\eta \ll r \ll L$; L is an integral length scale) result

$$\left\langle(\delta u^*)^n\right\rangle = C_{un}\, r^{*\frac{n}{3}}, \tag{2a}$$

when K41 is used (C_{un} is a universal constant). With K62,

$$\left\langle(\delta u^*)^n\right\rangle = C^{\dagger}_{un}\, r^{*\zeta_{un}}, \tag{2b}$$

where the exponents ζ_{un} may depart from $n/3$ due to the effect of intermittency in the dissipation rate ($C^{\dagger}_{un}$ may differ slightly from C_{un}).

An important "exact" relation between $\left\langle(\delta u)^2\right\rangle$ and $\left\langle(\delta u)^3\right\rangle$ was obtained by Kolmogorov [37], starting with the Karman–Howarth [35] equation for homogeneous isotropic turbulence,

$$-\left\langle(\delta u)^3\right\rangle = 4/5\langle\varepsilon\rangle r - 6\nu\frac{d}{dr}\left\langle(\delta u)^2\right\rangle. \tag{3}$$

A detailed derivation of Eq.(3) was provided by Batchelor [11]. More recently, the assumptions underlying the Kolmogorov equation have been revised [26,41] and formalized more rigorously [32]. A matched asymptotic expansion approach has been used by Lundgren [44] to obtain the same result. In the inertial range, the viscous term can be neglected and (3) reduces to the 4/5 law, viz.

$$-\left\langle(\delta u)^3\right\rangle = (4/5)\langle\varepsilon\rangle r \quad \text{or} \quad -\left\langle(\delta u^*)^3\right\rangle = (4/5)r^*\ . \tag{4}$$

It is important to underline that (3) and (4), as well as the hypotheses in K41 and K62, apply only at very large Reynolds numbers. It is not surprising, therefore, that for flows normally encountered in the laboratory, Eq.(1) appears to be satisfied only in the dissipative range (typically $r^* \le 10$) (see §7 of [19] and [53]); although the evidence is not altogether convincing especially when the isotropic form of $\langle\varepsilon\rangle$, viz

$$\langle\varepsilon\rangle_{\rm iso} = 15\nu\left\langle\left(\partial u/\partial x\right)^2\right\rangle \tag{5}$$

is used in forming δu^* and r^*. With a few exceptions, the laboratory data also indicate an asymptotic approach to Eq.(2a) (or Eq.(2b)) and Eq.(4) as the Reynolds number (usually represented by R_λ and defined by $\left\langle u^2\right\rangle^{\frac{1}{2}}\lambda/\nu$, where λ is the Taylor microscale $\left\langle u^2\right\rangle^{\frac{1}{2}}/\left\langle\left(\partial u/\partial x\right)^2\right\rangle^{\frac{1}{2}}$) increases. When R_λ is finite, deviations from Eqs.(2), (4) and indeed (5) can be quite significant. When R_λ is fixed, the deviations may also depend on the nature of the flow, thus casting doubt on any claim of universality. For the same flow and R_λ, departures from Eqs.(2) and (5) can still depend on the initial conditions that are used. It seems reasonable to ascribe these deviations to a lack of homogeneity in laboratory flows, the source of inhomogeneity depending on a number of parameters, such as the Reynolds number, type of flow and initial conditions.

In deriving Eq.(3), Kolmogorov ignored the nonstationary or nonhomogoneous term (space or time derivative term, respectively). This term has since been considered by a number of authors (e.g., Danaila et al [21], Lindborg [41], Qian [54,55], Lundgren [43]) in the context of decaying homogeneous isotropic turbulence. There have also been attempts at identifying this nonstationarity in more complicated flows, e.g. the centreline region of a fully developed channel flow (Danaila et al. [22]), a homogeneous uniform shear flow (Casciola et al. [18], Danaila et al. [20], Qian [55,56]) and the region near the axis of a circular jet (Danaila et al. [24]). Forcing has been used in physical experiments (e.g., Moisy et al. [46]) to achieve stationarity. Stationary isotropic turbulence is often studied numerically by adding a forcing term to the Navier–Stokes equation (e.g., [26,30]).

It should also be recalled that, at the relatively large Reynolds numbers which occur in the atmospheric surface layer, the evidence in support of the "4/5" law is rather inconclusive. This is partly due to the uncertainty in estimating $\langle\varepsilon\rangle$. The data of Sreenivasan and Dhruva [60] for $R_\lambda \simeq 10^4$ indicated, however, that there is no discernible range over which $d\langle(\delta u)^3\rangle/dr$ is constant over a convincing range. This raises some concern since the existence of the inertial range has been traditionally linked to the linear increase of $\langle(\delta u)^3\rangle$ with r. These authors further noted that an inertial range could not be identified unambiguously from the local slopes of the even-order moments of δu. They also stressed the difficulty of discussing the scaling of $\langle(\delta u)^n\rangle$ effectively without first understanding the effects of finite shear and finite R_λ. The previous observations can only fuel speculation about the meaningfulness of the scaling exponents that have been inferred from laboratory data and also the corresponding inferences regarding the departures of these exponents from the K41 predictions. For example, Lindborg [41] noted that "in order to test intermittency theories experimentally, it is necessary to recover Kolmogorov's law with good accuracy in a sufficiently broad range of scales. Otherwise there is no reason to put faith in possible observed deviations from the K41 theory".

In this paper, the focus is almost exclusively on the effect the inhomogeneity has on what is loosely referred to as the scaling range or restricted scaling range. We adopt the approach previously used by Danaila et al. [21–23], which consists in extending Eq.(3) to a statement which, in essence, expresses a scale-by-scale energy budget for a particular flow. Previously published data as well as new measurements for grid turbulence and along the axis of a circular jet are examined with the aim of quantifying possible differences in the inhomogeneity among various flows. Specifically, we distinguish between flows which are dominated by the decay of turbulent energy along the main flow direction—such as grid turbulence, jets and wakes—and flows which have been forced. In experiments, forcing can be achieved by stirring the flow with moving boundaries [46], introducing body forces or with zero-net mass-flow-rate jets [14,32]. In numerical simulations, it is usually achieved by continuously injecting energy at low wavenumbers [30]. We also examine how the asymptotic K41 result may be reached in these two flow categories.

Inhomogeneity in Decaying and Forced Flows

In this section, we give examples of how the inhomogeneity can affect relation (3) in decaying flows. The modified form of this relation can be written as

$$-\langle(\delta u)^3\rangle = 4/5\langle\varepsilon\rangle r - 6\nu\frac{d}{dr}\langle(\delta u)^2\rangle + I_u \tag{6}$$

where I_u represents the inhomogeneity associated with the large scale motion. For decaying grid turbulence, [21]

$$I_u \equiv 3U/r^4\int_0^r \omega^4\frac{d}{dx}\langle(\delta u)^2\rangle d\omega \tag{7a}$$

where U is the mean velocity in the x direction and ω a dummy integration variable. For forced turbulence, Moisy et al [46] obtained (using [51])

$$I_u \equiv -2/7\langle\varepsilon\rangle r^3/L_f\,, \tag{7b}$$

where L_f is an integral scale which characterises the forcing. A similar expression is given by Gotoh et al [30] and Fukayama et al [26]. Since I_u is negative, its presence in Eq.(6) is to keep the magnitude of $-\langle(\delta u)^3\rangle$ below its asymptotic value of $4\langle\varepsilon\rangle/5$. As a consequence, measured values of $-\langle(\delta u^*)^3\rangle$ cannot exceed $4r^*/5$, unless $\langle\varepsilon\rangle$ is evaluated incorrectly. Note that Eq.(6) should provide a more reliable indirect means of estimating $\langle\varepsilon\rangle$.

A more general form of Eq.(6) is the corresponding transport equation for the energy structure function $\langle(\delta q)^2\rangle \equiv \langle(\delta u)^2\rangle + \langle(\delta v)^2\rangle + \langle(\delta w)^2\rangle$ (v and w are velocity fluctuations in the y and z directions, respectively), e.g. [24],

$$-\langle\delta u(\delta q)^2\rangle = 4/3\langle\varepsilon\rangle r - 2\nu\frac{d}{dr}\langle(\delta q)^2\rangle + I_q \tag{8}$$

with

$$I_q \equiv (2U/r^2)\int_0^r \omega^2\frac{d}{dx}\langle(\delta q)^2\rangle d\omega \tag{9}$$

for decaying homogeneous isotropic turbulence. Note that now 4/5 has been replaced by 4/3. One advantage of Eq.(8) over Eq.(6) is that it allows a more meaningful comparison with the transport equation for $\langle(\delta\theta)^2\rangle$, where θ is the scalar fluctuation (e.g. [3]). Another advantage, [21], is that, for small r, it is consistent with a more general form of $\langle\varepsilon\rangle$ than $\langle\varepsilon\rangle_{\text{iso}}$, i.e.

$$\langle\varepsilon\rangle_q = 3\nu\langle(\partial u/\partial x)^2 + (\partial v/\partial x)^2 + (\partial w/\partial x)^2\rangle \tag{10}$$

whereas, at sufficiently large r, it reproduces the turbulent energy budget, viz.

$$\langle\varepsilon\rangle = -\frac{U}{2}\frac{d\langle q^2\rangle}{dx} \tag{11}$$

(without the need to assume isotropy at large scales, i.e. $\langle q^2\rangle = 3\langle u^2\rangle$; such an assumption is invalidated in most grid turbulence experiments because $\langle u^2\rangle$ is typically larger than $\langle v^2\rangle$ or $\langle w^2\rangle$ by nearly 20%). As noted by Antonia et al [9], the presence of I_u in Eq.(6), or I_q in Eq.(8), allows compliance with two important classical results. The energy budget is retrieved at large r, whilst the decay of $\langle\varepsilon\rangle$ or, equivalently, the enstrophy in homogeneous turbulence, is correctly reproduced in the limit of $r \to 0$.

For reasons mentioned above we have preferred to validate Eq.(8), instead of Eq.(6), using (new) measurements obtained in grid turbulence and along the axis of a circular jet. Both these flows offer advantages in the present context. In grid turbulence, $\langle\varepsilon\rangle$ can be inferred reliably from Eq.(11); from an experimental viewpoint, this can be exploited usefully, e.g. for assessing any possible degradation to the high wavenumber part of the spectrum, e.g. [57]. Along the axis of a circular jet it can be shown that the structure functions should satisfy similarity, when normalized by the energy and Taylor microscale [16]. Because R_λ is constant along the axis, other combinations of normalising scales, such as (η, u_K^2) and ($L, \langle q^2\rangle$), should also result in the collapse of the structure functions.

Experimental Details

The grid turbulence tunnel has a working section of $350\,\text{mm} \times 350\,\text{mm}$ and is $2.4\,\text{m}$ long. A biplane square mesh

grid ($M = 24.8$ mm with 4.76 mm square rods and a solidity of 0.35) is placed at the entrance section and measurements are made on the centreline at $x = 52M$, where the turbulence is approximately locally homogeneous and isotropic. The mean streamwise velocity is about $6\,\mathrm{ms}^{-1}$.

The jet exits from a contraction (85:1 area ratio). The exit diameter, *D*, is 55 mm. Data are taken on the axis, at a distance of 40*D* downstream of the exit, where the mean velocity in the streamwise direction is about $4.5\,\mathrm{ms}^{-1}$.

The velocity was measured with in-house hot wires, operated with in-house constant temperature anemometer circuits. The hot wire (Pt−10% Rh) was etched to a diameter of d_w of 2.5μm and an active length l_w so that the ratio l_w/d_w was approximately 200. The CTA circuits were operated at an overheat ratio of 1.5, with a cut-off frequency set at approximately 15 kHz. The sampling frequency, f_s, was 8kHz for the grid turbulence and 12.6kHz for the jet measurements while the analog filters were set at f_s/2. The anemometer signals were digitized into a PC using a 16-bit AD board. The geometrical angle between the wires was nearly 90°. The calibration of the X-wire was performed using a look-up-table (LUT) method [15]. A comparison between LUT and the effective angle method showed that the former gives more reliable results when the velocity is below about $6\mathrm{ms}^{-1}$. With LUT, the velocity and velocity derivative statistics, in both grid turbulence and the far field of the circular jet, were in closer (but far from perfect) agreement with isotropy than when the effective angle calibration was used. Corrections for the spatial attenuation of the hot-wires (using the method outlined in Zhu and Antonia [64]) and Taylor's hypothesis (following [34]) have been applied.

Comparison of Experimental and Numerical Data with Eqs.(6) and (8)

All the measured terms in Eq.(8) are shown in Fig.1 (grid turbulence) and Fig.2 (jet axis). All terms have been normalized by dividing by $\langle\varepsilon\rangle r$. The determination of $\langle\varepsilon\rangle$, as given by Eq (10), has been used in each case. For grid turbulence, $\langle\varepsilon\rangle_q$ was within 5% of the value estimated from measurements of $\langle q^2\rangle$ via Eq (11). Use of $\langle\varepsilon\rangle_{\mathrm{iso}}$ resulted in Eq (11) being satisfied within 10%. In the jet experiment, $\langle\varepsilon\rangle_q$ was in satisfactory (5%) agreement with the measured energy budget along the axis. This budget included turbulent advection and production via the normal stresses (the turbulent diffusion was found to be negligible) but ignored the pressure diffusion term; although justification for this latter assumption is lacking, the use of $\langle\varepsilon\rangle_{\mathrm{iso}}$, instead of $\langle\varepsilon\rangle_q$, resulted in a 17% imbalance in the budget for $\langle q^2\rangle$). In estimating I_q use was made of similarity [7], viz.

$$\langle\delta q^2\rangle = \langle q^2\rangle\, f(r/\lambda) \tag{12}$$

$$-\langle\delta u(\delta q)^2\rangle = \langle q^2\rangle^{\frac{3}{2}}\, g(r/\lambda) \tag{13}$$

For grid turbulence, where f and g determine the shape of the structure functions and are dependent only on r/λ (not on *x*),

$$I_q \equiv \underbrace{(U/r^2)\langle q^2\rangle\lambda^2\frac{d\lambda}{dx}\int_0^{r/\lambda}(\omega/\lambda)^3 f'd(\omega/\lambda)}_{I_{q_2}} + \underbrace{(U/r^2)\lambda^2\frac{d\langle q^2\rangle}{dx}\int_0^{r/\lambda}(\omega/\lambda)\, f\, d(\omega/\lambda)}_{I_{q_1}}. \tag{14}$$

On the jet axis, I_q is given by

$$I_q \equiv I_{q_1} + I_{q2} + \underbrace{(2/r^2)\frac{dU}{dx}\langle q^2\rangle\lambda^3\int_0^{r/\lambda}(\omega/\lambda)^2(e-h)\,d(\omega/\lambda)}_{I_{q3}} \tag{15}$$

where I_{q1} and I_{q2} are indicated in Eq (14). The prime denotes a derivative with respect to the similarity variable (ω/λ). The extra term (I_{q_3}) represents the contribution from the difference between the longitudinal and radial structure functions, viz.

$$\langle(\delta u)^2\rangle = \langle q^2\rangle\, e(r/\lambda) \tag{16}$$

$$\langle(\delta v)^2\rangle = \langle q^2\rangle h(r/\lambda). \tag{17}$$

In forming $\langle(\delta q)^2\rangle$, we have assumed that $\langle(\delta v)^2\rangle = \langle(\delta w)^2\rangle$ so that $\langle(\delta q)^2\rangle = \langle(\delta u)^2\rangle + 2\langle(\delta v)^2\rangle$ and consequently $\langle v^2\rangle = \langle w^2\rangle$, so that $\langle q^2\rangle = \langle u^2\rangle + 2\langle v^2\rangle$. Justification for the similarity scales $\langle q^2\rangle$ and $\langle\lambda\rangle$ was provided by George [29] who considered the spectral equations for decaying homogeneous isotropic turbulence and also Antonia et al. [7] and Danaila et al. [23] who considered the transport equation for $\langle(\delta q)^2\rangle$.

In the jet, the first term of Eq.(14), I_{q1}, involving the decay of $\langle q^2\rangle$, was estimated after applying a least squares fit to the axial profiles of $\langle q^2\rangle$ over the range $38 \le x/D \le 42$. The decay of the mean velocity was estimated in the same way, for the last term I_{q3}. Finally, a fit to the streamwise variation of λ was used to estimate I_{q2}. A more general definition of λ_q ($= 5\nu\langle q^2\rangle/\langle\varepsilon\rangle_q$, and consequently $R_\lambda = \langle q^2\rangle^{1/2}\lambda_q/3^{1/2}\nu$ [2]), which takes into account the three velocity components, has been used in analysing these data.

The linear vertical scale in Figs 1 and 2 provides a more severe test of how closely Eq.(8) is satisfied by the measurements than the logarithmic scale used in previous papers [9,51]. The imbalance, or difference between 4/3 and the remaining normalized terms in Eq.(8), is satisfactory, especially for Fig.1. The imbalance (dashed lines in Figs. 1 and 2) is larger for the jet than for grid turbulence. There may be several reasons for this. More assumptions were made [24] in the derivation of Eq.(15) than for Eq.(7a). The turbulence intensity in the jet is about 25%, much larger than that for grid turbulence (2.5%). This may introduce an additional uncertainty due to the use of Taylor's hypothesis (although modified, following [34]) and the neglect of the binormal component (the out-of-plane velocity component not resolved by the X-wire).

It is noteworthy, however, that at $r \approx \lambda_q$ the balance is almost exact, implying that $\langle\varepsilon\rangle$ can be estimated from Eq.(8), once the second- and third-order structure functions are known. The major difference between Figs 1 and 2 reflects, to a large extent, the higher value of R_λ in the jet. Correspondingly, the maximum

value of $-\left\langle \delta u(\delta q)^2 \right\rangle / \langle \varepsilon \rangle r$ is twice as large in Fig.2 than in Fig.1. Accordingly, the likelihood of a scaling range is bigger for Fig.2 than Fig.1. This range can be very roughly inferred from the intersections of the distribution corresponding to this term with those for the viscous term and for I_q. The locations of these crossings are denoted by r_ℓ and r_h in the figures. The difference $(r_h - r_\ell)$ is significant in Fig.2 but negligible in Fig.1, so that a scaling range would be most tenuous for Fig.1. The separate contributions to I_q are also included in Figs 1 and 2. The major contribution comes from I_{q_1}, the term associated with the streamwise decay of $\langle q^2 \rangle$; in this sense, the central region of the jet resembles grid turbulence for which this is the dominant term (see Eq.(8)). One may expect a similar behaviour to apply along the centreline of wakes, but not in a pipe or a channel, because of the streamwise inhomogeneity; here, the effect of turbulent diffusion along the wall-normal direction cannot be ignored. The contributions from I_{q_2} are not negligible around $r \approx \lambda_q$ (Fig.1) and $r \approx 10\lambda_q$ (Fig.2). I_{q_3} becomes largest at the largest r/λ_q.

The DNS data for box turbulence of Fukayama et al. [26] (replotted here on a linear scale) are shown in Fig.3. Results for both decaying and forced turbulence, obtained at the same $R_\lambda (\simeq 70)$, are included. There is almost no difference between the viscous terms, reflecting the normalization by η (e.g., [2]). The maximum value of $-\langle (\delta u)^3 \rangle / \langle \varepsilon \rangle r$ is larger for forced turbulence, reflecting the smaller value of I_u in this case. The difference between the forced and decaying values of I_u is only likely to increase, as R_λ is increased. Unfortunately, DNS data for decaying box turbulence at large R_λ are not yet available. That the influence of I_u (or I_q) on scales corresponding to the peak in $-\langle (\delta u)^3 \rangle / \langle \varepsilon \rangle r$ should diminish as R_λ increases can be readily inferred from available data in decaying grid turbulence. The data in [62] are reproduced in Fig. 4; although the R_λ range is limited, the trend is unmistakable. The magnitude of I_u, estimated here from the measured values of $\langle (\delta u^*)^2 \rangle$ and $\langle (\delta u^*)^3 \rangle$ and assuming the validity of Eq.(5), decreases with R_λ at least as rapidly as that of the viscous term.

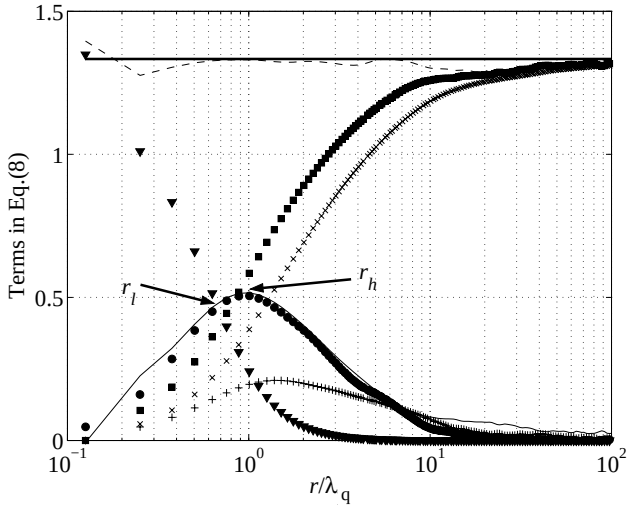

Figure 1: Terms in Eq.(8), divided by $\langle \varepsilon \rangle r$, for grid turbulence ($R_\lambda \approx 50$). ▼, viscous term; ●, third-order structure function; ■, I_q; ×, I_{q1}; +, I_{q2}; solid line: calculated third-order structure function using Eq.(8); solid thick line: 4/3; dashed line: sum of the viscous term, third-order structure function term and I_q.

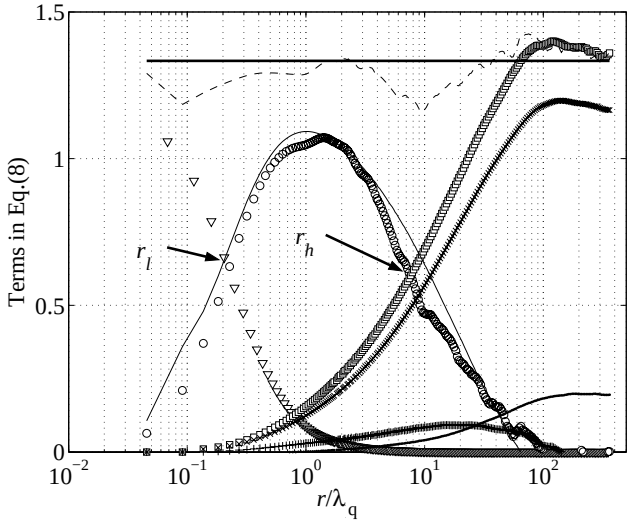

Figure 2: Terms in Eq.(8), divided by $\langle \varepsilon \rangle r$, for the jet ($R_\lambda \approx 363$). ▽, viscous term; ○, third-order structure function; □, I_q; ×, I_{q1}; +, I_{q2}; ····, I_{q3}; solid line: calculated third-order structure function using Eq.(8); solid thick line: 4/3 limit; dashed line: sum of the viscous term, third-order structure function term and I_q.

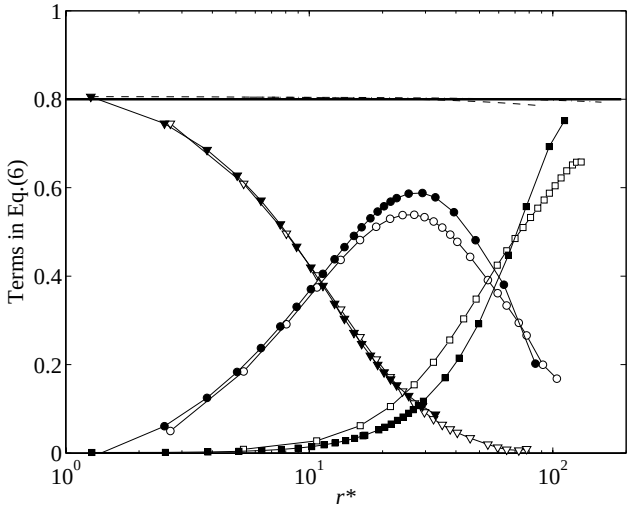

Figure 3: Terms in Eq.(6), divided by $\langle \varepsilon \rangle r$, using the DNS data of Fukayama et al [26] at roughly the same $R_\lambda (\simeq 70)$. Filled-in symbols: forced turbulence; open symbols: decaying turbulence. ○, ●: third-order structure function; ■, □: I_q; ▼, ▽: viscous term; dashed line: sum of the viscous term, third-order structure function term and I_q.

For a fixed R_λ, I_u (or I_q) may not be universal, even within the same flow type. For example, in the similarity region of decaying grid turbulence, the shape of the normalized form of I_q has been found to depend on the geometry of the grid [40]. A less sensitive dependence on the initial condition at the nozzle exit of a round jet has been reported in [17]. In this case the third-order structure functions, in the far field of the jet, remained unchanged under modified initial conditions. For the wake data of [10] (where 5 wake generators were used), Fig.5, I_u was inferred indirectly from measurements of $\langle (\delta u)^2 \rangle$ and $\langle (\delta u)^3 \rangle$ by assuming the validity of Eq.(6). Although R_λ is nominally constant in Fig.5, the peak of $-\langle (\delta u)^3 \rangle / \langle \varepsilon \rangle r$ and the magnitude of I_u exhibit significant variations as the initial conditions are changed. It can be argued that different levels of large scale organisation in each flow can lead to differences in I_u, and they can produce differences in the departure from the 4/5 law. It is not difficult to

imagine that such departures can be reflected in differences in scaling exponents (e.g., [10]). The reasonable collapse of the viscous term in Fig.5 reflects mainly the constant value of R_λ; an improved collapse at small r would be expected if r is normalized by η rather than λ. The lack of collapse of the third-order structure term in Fig.5 seems all the more significant given that, in each wake, R_λ is constant along x, so that a similarity based on λ seems appropriate.

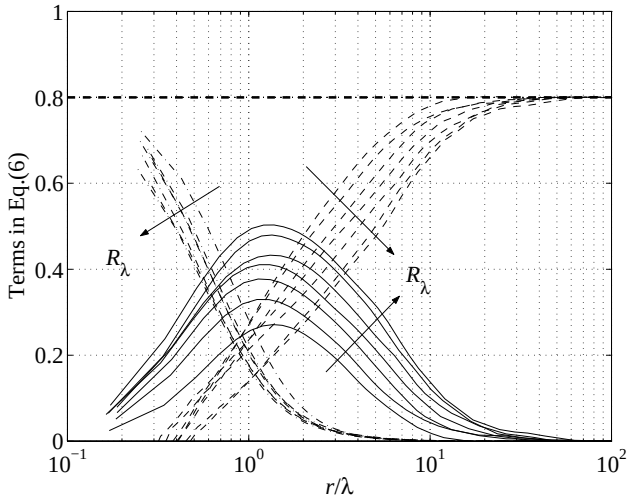

Figure 4: Variation with R_λ of the terms in Eq.(5), divided by $\langle\varepsilon\rangle r$, for the grid turbulence data of [62] (R_λ increases between 27 and 100 in the direction of the arrows). Solid line: $-\left\langle\left(\delta u^*\right)^3\right\rangle r^{*-1}$; dashed line: I_u (calculated by difference from Eq.(6)); dash-dotted line: viscous term; dashed horizontal line: 4/5.

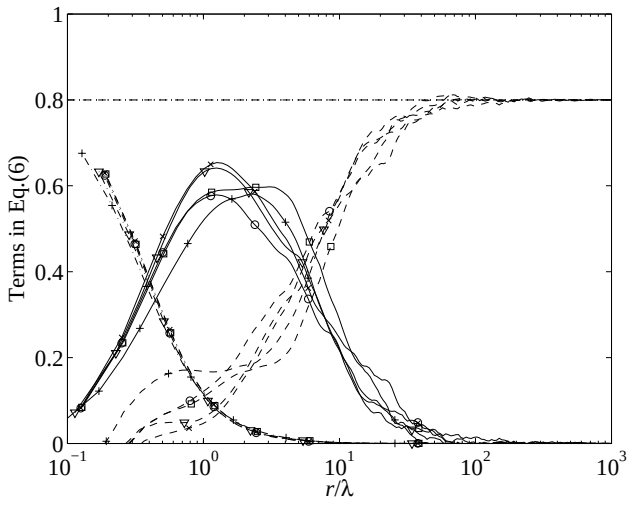

Figure 5: Terms in Eq.(6), divided by $\langle\varepsilon\rangle r$, for the turbulent wake data of [10] at nominally the same $R_\lambda(\approx 200)$. □: plate; ○: circular cylinder. ▽: square cylinder; ×: screen cylinder; +: screen strip; solid line: third-order structure function; dash-dotted line: viscous term; dashed line: inhomogeneous term, calculated by difference from Eq.(6); dash-dotted horizontal line: 4/5.

Distributions of $-\left\langle\delta u\left(\delta q\right)^2\right\rangle$ were calculated from Eq.(8) starting with the measured distributions of $\left\langle\left(\delta q\right)^2\right\rangle$ and assuming similarity based on λ and $\left\langle q^2\right\rangle$. The agreement between these calculations (solid lines in Figs. 1 and 2) and the measurements is quite satisfactory, providing some indirect support for the validity of Eq.(8) and the assumptions made in estimating its terms.

Extrapolation to Large R_λ

Clearly, it is important to ascertain how quickly the maximum value of $-\left\langle\delta u\left(\delta q\right)^2\right\rangle$ divided by $\langle\varepsilon\rangle r$ or $\left\langle(\delta u)^3\right\rangle$ divided by $\langle\varepsilon\rangle r$ approaches its asymptotic value of 4/3 or 4/5. This has been the objective of many investigations. Our main interest here is to examine the R_λ dependence of this term in conjunction with that for the viscous and inhomogeneous terms in Eq.(8). To this end, we follow the approach by Antonia et al. [7] who used a description of $\left\langle(\delta u^*)^2\right\rangle$ [25,39] which extends from the smallest (Kolmogorov) scale to the integral scale L,

$$\left\langle(\delta u^*)^2\right\rangle = \left(r^{*2}/15\right)(1+\beta r^*)^{2c-2}/(1+(r^*/r_{cu}^*)^2)^c \tag{18}$$

where r_{cu}^* is identified with the crossover between the dissipative and inertial ranges, $c \equiv (1-\zeta_u/2)$ and $\beta \equiv L^{*-1}$. Eq.(18) is essentially a modification, for finite Reynolds numbers, of the model for $\left\langle(\delta u^*)^2\right\rangle$ first proposed by Batchelor [12] with β=0. To obtain $\left\langle(\delta q^*)^2\right\rangle$, use is made of the isotropic relation

$$\left\langle\left(\delta q^*\right)^2\right\rangle = \left(3 + r^*\frac{d}{dr^*}\right)\left\langle\left(\delta u^*\right)^2\right\rangle. \tag{19}$$

For isotropic turbulence, $\lambda^* = 15^{1/4}R_\lambda^{1/2}$, $\left\langle q^{*2}\right\rangle = \left(3/15^{1/2}\right)R_\lambda$ and $L^* \equiv 15^{-3/4}C_\varepsilon R_\lambda^{3/2}$, where L has been identified with $C_\varepsilon\left\langle q^2\right\rangle^{3/2}/\langle\varepsilon\rangle$. The dimensionless energy dissipation rate parameter C_ε is expected to become constant at sufficiently large R_λ but its magnitude should depend on the initial conditions. This is true in both experiments, e.g. [4], or simulations, e.g. [58] and references therein. In general, one expects the shape of $\left\langle(\delta u^*)^2\right\rangle$ $\left(\text{and}\left\langle\left(\delta q^*\right)^2\right\rangle\right)$ to depend on the type and level of organisation in a particular flow (e.g. [40]), which may in any case reflect the influence of the initial conditions. Here, we have assumed a value of 1 for C_ε, as in [7]. We have also assumed that $r_{cu}^* \equiv (15C_{u2})^{3/4}$, with a value of 2 for the Kolmogorov constant C_{u2}. The K41 value of 2/3 was assigned to ζ_u, i.e. intermittency was ignored (calculations taking into account intermittency on $\left\langle(\delta u^*)^2\right\rangle$ did not show significant differences). Although C_{u2}, ζ_u and r_{cu}^* may vary slowly with R_λ (e.g. [5]) at small R_λ we believe that the present estimates of I_u (or I_q) and $-\left\langle(\delta u)^3\right\rangle$ (or $-\left\langle(\delta u)(\delta q)^2\right\rangle$) should be sufficiently reliable to provide a first-order indication of how the Kolmogorov's asymptotic result may be approached. Calculations of $-\left\langle(\delta u)^3\right\rangle/\langle\varepsilon\rangle r$ are shown in Fig.6 together with those for the viscous term and I_u in Eq.(6). As R_λ increases, the latter two distributions shift to the left and right respectively, thus increasing the relevance of an inertial range. Nonetheless, the attainment of such a range requires values of R_λ well in excess of $R_\lambda = 10^4$. Even at $R_\lambda = 10^6$, it would appear that the extent of this range is limited; the difference between $-\left\langle(\delta u)^3\right\rangle/\langle\varepsilon\rangle r$ and 4/5 is smaller than 1% over $\simeq 2.8$ decades in r/λ but the shape

of $-\left\langle(\delta u)^3\right\rangle/\langle\varepsilon\rangle r$ indicates that this quantity exhibits a maximum. Perhaps not surprisingly, $\left\langle\left(\delta u^*\right)^2\right\rangle/r^{*-2/3}$ appears to reach its assumed asymptotic value of 2 (the Kolmogorov constant) at $R_\lambda \simeq 10^4$ (Fig.7). The grid turbulence data ($R_\lambda = 100$) of Zhou & Antonia [62] have been included to show that relation (18) approximates the measured data adequately.

The variation with R_λ of the calculated maximum value of $-\left\langle\left(\delta u^*\right)^3\right\rangle r^{*-1}$ is shown in Fig.8. The calculation (solid line) is in good agreement with measurements obtained in grid turbulence and along the centreline of a circular jet (note that here the 4/3 value has been rescaled to 4/5 for our data). The plane jet data of Pearson and Antonia [53] lie below this line, partly because $\langle\varepsilon\rangle_{\rm iso}$ has been used instead of $\langle\varepsilon\rangle_q$. For the jet and grid turbulence data of [28], $\langle\varepsilon\rangle_{\rm iso}$ was used. The large scatter associated with the active grid turbulence data of [48] may in part reflect the uncertainty in the estimation of $\langle\varepsilon\rangle$ in this experiment. The above comments suggest that, evidently, caution is required when interpreting the good agreement of most of the experimental decaying turbulence data with the model. The model is unlikely to take fully into account the differences in the initial conditions that have been found to exist between different experiments. The variation in the peak value of $-\left\langle\left(\delta u^*\right)^3\right\rangle r^{*-1}$ for various wake data (fig.5), at nominally the same R_λ, supports the idea that a universal distribution is unlikely. This idea is consistent with the view (e.g., [30]) that simple shear flows do not reach universal asymptotic states. The results from the model are in close agreement with the prediction (dash-dotted line) of Lundgren [43] for $R_\lambda \gtrsim 200$. For lower values of R_λ, the model based on Eq.(18) is in satisfactory agreement with the grid turbulence data of [62] (the difference between $\langle\varepsilon\rangle_{\rm iso}$ or $\langle\varepsilon\rangle_q$ and the value of $\langle\varepsilon\rangle$ estimated with Eq.(11) is quite small for these data). The measured and numerical data obtained in forced turbulence (denoted by filled-in symbols) seem to follow a separate distribution (it is unlikely that this distribution is unique in view of the documented effects if initial conditions for this type of turbulence); clearly the approach to 4/5 is much more rapid for these data and a value of 10^3 for R_λ may be sufficient for this type of turbulence to reach the Kolmogorov asymptote. This value is somewhat larger than the maximum value ($\simeq 460$) for DNS data of Gotoh et al. [31]; this may need to be kept in mind when assessing DNS data with forcing. For decaying turbulence, a value of R_λ in excess of 10^5 (perhaps even 10^6) may be needed before the K41 asymptotic state is reached. This estimate is somewhat higher than that given in [63] where the Batchelor parameterization was used for modelling $\left\langle(\delta u^*)^2\right\rangle$.

The difference between r_h and r_ℓ is of interest when enquiring into the possible existence of a scaling range. Fig.9 indicates that $\log(r_h/r_\ell)$ varies linearly with $\log R_\lambda$. For $R_\lambda \geq 10^4$, this range is equivalent to considering 50% of the maximum of $-\left\langle\left(\delta u^*\right)^3\right\rangle r^{*-1}$. Qian [54] adopted a slightly different criterion for identifying the extent of the inertial range, but obtained a similar linear dependence on R_λ (his figure 8). We recognize that there is inevitable arbitrariness in the definition of a scaling range; nonetheless, the dash-dotted line in Fig.9 indicates that R_λ should exceed 3×10^5 to achieve a 2 decades plateau in $-\left\langle\left(\delta u^*\right)^3\right\rangle r^{*-1}$.

The inset in Fig.9 shows that the location of the maximum of $-\left\langle\left(\delta u^*\right)^3\right\rangle r^{*-1}$ approaches a constant value for $r \simeq 1.1\lambda$. This trend appears to have been established for decaying turbulence [28,43,62]. However, Lundgren [43] showed that, in the case of linearly forced turbulence, the maximum is at a higher value, $r \simeq 1.23\lambda$, implying a different behaviour for forced turbulence.

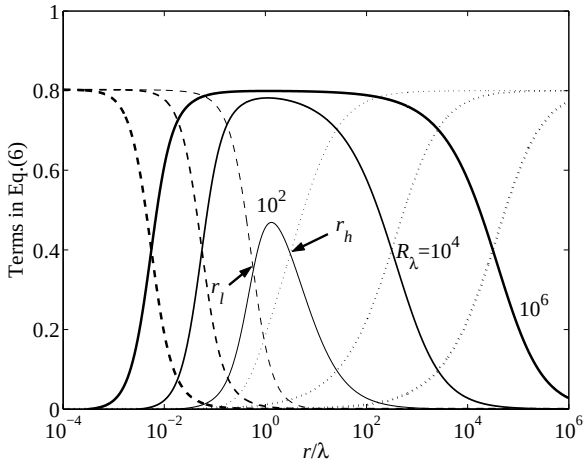

Figure 6: Variation with R_λ of the terms in Eq.(6), divided by $\langle\varepsilon\rangle r$, derived from a model of decaying isotropic turbulence, Eq.(18). Solid line: third-order structure function; dotted line: I_u; dashed line: viscous term.

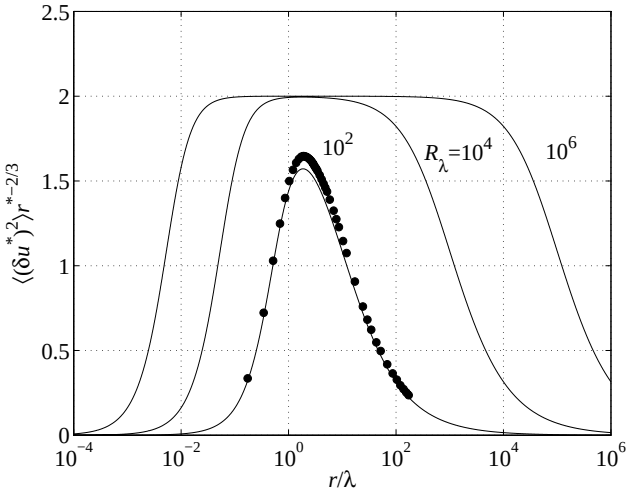

Figure 7: Kolmogorov-normalized second-order structure function of u, divided by $r^{*2/3}$. Solid lines: model Eq.(18); •, measured grid turbulence data of [62] at R_λ =100.

Concluding Comments

The limiting values of 4/5 and 4/3, which appear in the stationary form of the transport equations for $\left\langle(\delta u)^2\right\rangle$ and $\left\langle(\delta q)^2\right\rangle$, represent asymptotic states corresponding to large Reynolds numbers. For laboratory flows, deviations from these values can be significant; even in the atmospheric surface layer, the deviations may not be negligible. The inclusion of the non-stationarity or inhomogeneity (due mainly to the large scale motion) in the transport equation for $\left\langle(\delta u)^2\right\rangle$ and $\left\langle(\delta q)^2\right\rangle$ allows some assessment to be made on whether a scaling range, albeit of restricted extent, is possible. Experimental and numerical results obtained in a number of different flows indicate that the magnitude of the inhomogeneous term, I_u or I_q, can depend on various parameters, including initial conditions. In

particular, across the scaling range, the magnitude of I_u (or I_q) is smaller for forced than decaying-type turbulence. Consistently, the maximum value of $-\left\langle \left(\delta u^*\right)^3 \right\rangle r^{*-1}$ approaches 4/5 more rapidly, as R_λ is increased, in forced than in decaying-type turbulence. This trend seems to be convincingly supported by both measured and numerical data. Antonia and Orlandi [1] noted that significant differences also existed for statistics of small-scale passive scalar (θ) fluctuations between forced and decaying homogeneous isotropic turbulence. One would expect that the R_λ variation of the maximum value of $-\left\langle \left(\delta u^*\right)\left(\delta\theta^*\right)^2 \right\rangle r^{*-1}$ will exhibit a similar behaviour, in terms of the difference between forced and decaying-type turbulence, to that in Fig. 8.

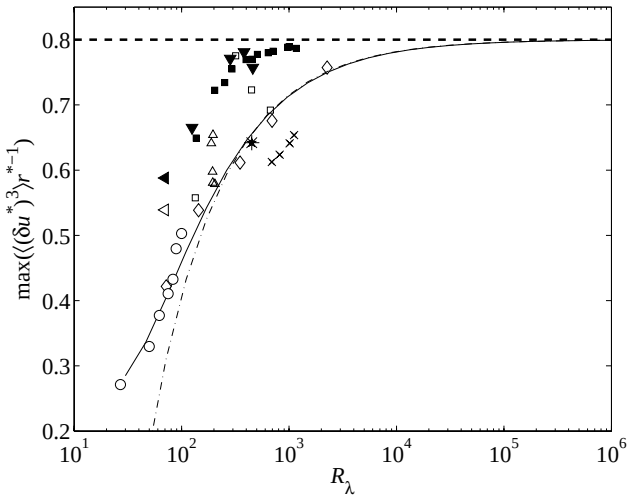

Figure 8: Variation with R_λ of the maximum of the normalized third-order structure function of u. Solid line: based on model Eq.(18); ▼, DNS data for forced box turbulence [30]; ◀, DNS data for forced box turbulence [26]; ◁, DNS data for decaying box turbulence [26]; ■, measured forced turbulence data [46]; ×, plane jet [53]; ○, grid turbulence [62]; ◊, values measured by [28]; *, round jet (present data); △, 2D wakes data [10]; dash-dotted line: model of [43]; □, grid turbulence [48]; dashed horizontal line: 4/5.

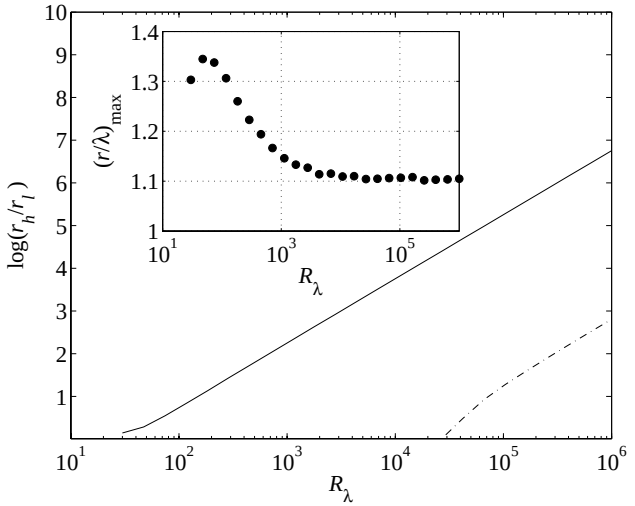

Figure 9: Dependence on R_λ of $\log(r_h/r_l)$, solid line. The dash-dotted line corresponds to a range where $-\left\langle \left(\delta u^*\right)^3 \right\rangle r^{*-1}$ is ≥99% of 4/5. Inset: location of the maximum value of the third-order structure function, divided by $\langle\varepsilon\rangle r$, as a function of R_λ.

Acknowledgements

The support of the Australian Research Council is acknowledged. We are especially grateful to L. Danaila for her major contributions to various aspects of this work, in particular the derivations of I_u in Eq.(7a) and I_q in Eq.(8).

References

[1] Antonia, R.A. and Orlandi, P., Effect of Schmidt Number on Small-Scale Passive Scalar Turbulence, *Appl. Mech Reviews*, **56**, 2003, 1-18.

[2] Antonia, R.A. and Orlandi, P., Similarity of Decaying Isotropic Turbulence with a Passive Scalar, *J. Fluid Mech.*, **505**, 2004, 123-151.

[3] Antonia, R.A., Ould-Rouis, M., Anselmet, F., Zhu, Y., Analogy between predictions of Kolmogorov and Yaglom. *J. Fluid Mech.*, **332**, 1997, 395-409.

[4] Antonia, R.A. and Pearson, B.R., Effect of Initial Conditions on the Mean Energy Dissipation Rate and the Scaling Exponent. *Phys. Rev. E* **62**, 2000, 8086-8090.

[5] Antonia, R.A., Pearson, B.R. and Zhou, T., Reynolds Number Dependence of Second-Order Velocity Structure Functions, *Phys. Fluids*, **12**, 2000, 3000-3006.

[6] Antonia, R.A. and Smalley, R.J., Scaling Range Exponents from X-wire Measurements in the Atmospheric Surface Layer, *Boundary-Layer Meteorology*, **100**, 2001, 439-457.

[7] Antonia, R.A., Smalley, R.J., Zhou, T., Anselmet, F., and Danaila, L., Similarity of energy structure functions in decaying homogeneous isotropic turbulence, *J. Fluid Mech.*, **487**, 2003, 245-269.

[8] Antonia, R.A., Zhou, T., Danaila, L. and Anselmet, F., Scaling of the mean energy dissipation rate equation in grid turbulence, *J. of Turbulence*, **3**, 2002, 034.

[9] Antonia, R.A., Zhou, T., Danaila, L. and Anselmet, F., Streamwise Inhomogeneity of Decaying Grid Turbulence, *Phys Fluids*, **12**, 2000, 3086-3089.

[10] Antonia, R.A., Zhou, T. and Romano, G.P., Small-Scale Turbulence Characteristics of Two-Dimensional Bluff Body Wakes, *J. Fluid Mech*., 2002, 67-92.

[11] Batchelor, G.K., Kolmogoroff's Theory of Locally Isotropic Turbulence, *Proc. Camb. Phil. Soc*., **43**, 1947, 533-559.

[12] Batchelor, G.K., Pressure Fluctuations in Isotropic Turbulence, *Proc. Camb. Phil. Soc.*, **47**, 1951, 359-374.

[13] Batchelor, G.K., *The Theory of Homogeneous Turbulence*, Cambridge University Press, Cambridge, Ma, 1953.

[14] Birouk, M., Sarh, B. and Gokalp, I., An attempt to realize experimental isotropic turbulence at low Reynolds number, *Flow Turbul. Comb*, **70**, 2003, 325-348.

[15] Burattini, P. and Antonia, R.A., The Effect of Different X-wire Calibration Schemes on some Turbulence Statistics, Accepted for publication in *Expts. in Fluids*, 2005.

[16] Burattini, P., Antonia, R.A. and Danaila, L., Similarity in the Far Field of a Turbulent Round Jet, Accepted for publication in *Phys. Fluids*, 2005.

[17] Burattini, P., Antonia, R.A. and Rajagopalan, S., Effect of initial conditions on the far field of a round jet, To appear in proceedings of *15 AFMC*, 2004.

[18] Casciola, C.M., Gualtieri, P., Benzi, R., Piva, R., Scale-by-scale budget and similarity laws for shear turbulence, *J. Fluid Mech.*, **476**, 2003, 105-114.

[19] Chassaing, P., Antonia, R.A., Anselmet, F., Joly, L and Sarkar, S., *Variable Density Fluid Turbulence*, Kluwer, 2002.

[20] Danaila, L., Anselmet. F., Zhou, T., Turbulent Energy Scale-Budget Equations for nearly Homogeneous Sheared Turbulence, *Flow Turbul. Comb.*, **72**, 2004, 287-310.

[21] Danaila, L., Anselmet, F., Zhou, T. and Antonia, R.A., A Generalization of Yaglom's Equation which accounts for the Large-scale Forcing in Heated Decaying Turbulence, *J. Fluid Mech.*, **391**, 1999, 359-372.

[22] Danaila, L., Anselmet, F., Zhou, T. and Antonia, R.A., Turbulent Energy Scale Budget Equations in a Fully Developed Channel Flow, *J. Fluid Mech.*, **430**, 2001, 87-109.

[23] Danaila L., Antonia, R.A. and Burattini, P., Progress in Studying Small Scale Turbulence using "exact" two-point equations. *New J. Phys*., **6**, 2004, 128.

[24] Danaila, L., Burattini, P., Antonia, R.A., Large-scale effects in a self-preserving, axisymmetric turbulent jet, 2004, In preparation.

[25] Dhruva, B., *An experimental study of high Reynolds number turbulence in the atmosphere*. PhD Thesis, 2000, Yale University.

[26] Frisch, U., *Turbulence: the Legacy of A.N. Kolmogorov*, Cambridge University Press, Cambridge, Ma, 1995.

[27] Fukayama, D., Oyamada, T., Nakano, T., Gotoh, T. and Yamamoto, K., Longitudinal structure functions in decaying and forced turbulence, *J. Phys. Soc. Jpn*., **69**, 2000, 701-716.

[28] Gagne, Y., Castaing, B., Baudet, C. and Malécot, Y., Reynolds Number Dependence of Third-order Velocity Structure Functions, *Phys. Fluids*, **16**, 2004, 482-485.

[29] George, W.K., The decay of homogeneous isotropic turbulence. *Phys. Fluids* A, 4, 1992, 1492-1509.

[30] George, W.K. and Davidson L., Role of initial conditions in establishing asymptotic flow behavior, *AIAA J*., **42**, 2004, 438-446.

[31] Gotoh, T., Fukayama, D. and Nakano, T., Velocity field statistics in homogeneous steady turbulence obtained using a high-resolution direct numerical simulation, *Phys. Fluids*, **14**, 2002, 1065-1081.

[32] Hill, R.J., Applicability of Kolmogorov's and Monin's equations of turbulence, *J. Fluid Mech.*, **353**, 1997, 67-81.

[33] Hwang, W. and Eaton, J.K., Creating homogeneous and isotropic turbulence without a mean flow, *Expts. in Fluids*, **36**, 444-454, 2004.

[34] Kahalerras, H., Malécot, Y., Gagne, Y. and Castaing, B., Intermittency and Reynolds number, *Phys. Fluids*, **10**, 1998, 910-921.

[35] von Karman, T and Howarth, L., On the Statistical Theory of isotropic turbulence, *Proc. R. Soc. London A*, 164, 1938, 192-215.

[36] Kolmogorov, A.N., The Local Structure of Turbulence in Incompressible Viscous Fluid for very Large Reynolds Numbers, *Dokl. Akad. Nauk. SSSR* **30,** 1941, 299-303.

[37] Kolmogorov, A.N., Dissipation of Energy in Locally Isotropic Turbulence, *Dokl. Akad Nauk SSSR*, **32,** 1941b, 9-21.

[38] Kolmogorov, A.N., A Refinement of Previous Hypotheses concerning the Local Structure of Turbulence in a Viscous Incompressible Fluid at High Reynolds Number, *J. Fluid Mech.*, **13**, 1962, 82-85.

[39] Kurien, K.S. and Sreenivasan, K.R. Anisotropic Scaling Contributions to High-Order Structure Functions in High Reynolds Number Turbulence. *Phys. Rev. E*, **62**, 000, 2206-2212.

[40] Lavoie, P., Antonia, R.A. and Djenidi, L., 2004. The Effect of Grid Geometry on the Scale-by-Scale Budget of Decaying Turbulence, To appear in proceedings of *15 AFMC*, 2004.

[41] Lindborg, E., A note on Kolmogorov's third-order structure function law, the local isotropy and the pressure-velocity correlation, *J. Fluid Mech.*, **326**, 1996, 343-356.

[42] Lindborg, E., Correction to the Four-fifths Law due to Variations of the Dissipation, *Phys. Fluids*, **11**, 1999, 510-512.

[43] Lundgren, T.S., Linearly Forced Turbulence, CTR Annual Research Briefs, 2003, 461-473.

[44] Lundgren, T.S., Kolmogorov Turbulence by Matched Asymptotic Expansion, *Phys. Fluids*, **15**, 2003, 1074-1081.

[45] Lundgren, T.S., Kolmogorov Two-thirds Law by Matched Asymptotic Expansion, *Phys. Fluids*, **14**, 2002, 638-642.

[46] Moisy, F., Tabeling, P. and Willaime, H., Kolmogorov Equation in a Fully Developed Turbulence Experiment, *Phys. Rev. Lett*., **82**, 1999, 3994-3997.

[47] Monin, A.S., and Yaglom A.M., *Statistical Fluid Mechanics*, vol. 2, 1975, MIT press, Cambridge, MA.

[48] Mydlarski, L., and Warhaft, Z., On the onset of high-Reynolds-number grid-generated wind tunnel turbulence, *J. Fluid Mech.*, **320**, 1996, 331-368.

[49] Nelkin, M., Universality and Scaling in Fully Developed Turbulence, *Advances in Physics*, **43**, 1994**,** 143-181.

[50] Nelkin, M., Turbulence in fluids, *Am. J. Phys.*, **68**, 2000, 310-318.

[51] Novikov, E.A., Statistical balance of vorticity and a new scale for vortical structures in turbulence, *Phys. Rev. Lett*., **71**, 1993, 2718–2720.

[52] Orlandi, P. and Antonia, R.A., Dependence of the Non-stationary Form of Yaglom's Equation on the Schmidt Number, *J. Fluid Mech*., **451**, 2002, 99-108.

[53] Pearson, B.R. and Antonia, R.A., Reynolds-number Dependence of Turbulent Velocity and Pressure Increments, *J. Fluid Mech*, **444**, 2001, 343-382.

[54] Qian, J., Inertial range and the finite Reynolds number effect of turbulence, *Phys. Rev. E*., **55**, 1997, 337-342.

[55] Qian, J., Slow Decay of the Finite Reynolds Number Effect of Turbulence, *Phys.Rev. E.*, **60,** 1999, 3409- 3412.

[56] Qian, J., Scaling of structure functions in homogeneous shear-flow turbulence, *Phys. Rev. E*, **65**, 2002, 036301.

[57] Schedvin, J.C., Stegen, G.R. and Gibson, C.H., Universal Similarity at High Grid Reynolds Numbers, *J. Fluid Mech*., **65**, 1974, 561-579.

[58] Sreenivasan, K., An update on the energy dissipation rate in isotropic turbulence, *Phys. Fluids*, **10**, 1998, 528-529.

[59] Sreenivasan, K.R. and Antonia, R.A., The Phenomenology of Small-scale Turbulence, *Ann. Rev. Fluid. Mech*., **29**, 1997, 435-472.

[60] Sreenivasan, K.R. and Dhruva, B., Is there scaling in High-Reynolds-Number Turbulence, *Prog. Theor. Phys. Suppl*., **130**, 1998, 103-120.

[61] Sreenivasan, K.R., Dhruva, B. and Gil, I.S., The Effects of Large Scales on the Inertial Range in High-Reynolds-Number Turbulence, 1999, eprint arXiv:chao-dyn/9906041.

[62] Zhou, T. and Antonia, R.A., Reynolds number dependence of the small-scale structure of grid turbulence, *J. Fluid Mech*., **406**, 2000, 81-107.

[63] Zhou, T., Antonia, R.A., Danaila, L. and Anselmet, F., Approach to the Four-fifths 'Law' for Grid Turbulence, *J. of Turbulence*, **1**, 2000, 005.

[64] Zhu, Y. and Antonia, R.A., Effect of Wire Separation on X-probe measurements in a Turbulent Flow, *J. Fluid Mech.*, **287**, 1995, 199-223.